

Photoelectron Spectroscopy of  $\text{CuO}^-$ <sup>†</sup>

Mark L. Polak, Mary K. Gilles, Joe Ho, and W. C. Lineberger\*

Joint Institute for Laboratory Astrophysics, University of Colorado and National Institute of Standards and Technology and Department of Chemistry and Biochemistry, University of Colorado, Boulder, Colorado 80309-0440 (Received: February 13, 1991)

Laser photoelectron spectroscopy has been used to study the  $\text{CuO}^-$  anion and neutral  $\text{CuO}$  molecule. Analysis of the photoelectron spectrum yields an electron affinity of 1.777 (6) eV for  $\text{CuO}$ . Equilibrium bond lengths and vibrational frequencies are obtained from a Franck-Condon analysis of the relative intensities of the observed transitions, yielding a  $\text{CuO}^-$  bond length of 1.670 (10) Å and a  $\text{CuO}^-$  vibrational frequency of 739 (25)  $\text{cm}^{-1}$ . The analysis also yields a bond length (1.704 (10) Å) and a vibrational frequency (682 (25)  $\text{cm}^{-1}$ ) for the  $Y^2\Sigma^+$  excited state of  $\text{CuO}$ .

## Introduction

Although neutral diatomic transition-metal monoxides have been the subject of extensive spectroscopic investigation,<sup>1,2</sup> very little is known about the corresponding anions. To our knowledge there have been no reports of molecular parameters (i.e., bond lengths, vibrational frequencies, electron detachment energies, etc.) for these anions, with the exception<sup>3</sup> of  $\text{FeO}^-$ . In addition, ab initio studies of these metal monoxides have generally been confined to the neutral molecule or the corresponding cation.

Copper monoxide ( $\text{CuO}$ ), and the corresponding anion,  $\text{CuO}^-$ , are no exception to this pattern. The electronic spectra and structure of  $\text{CuO}$ , both experimentally and theoretically determined, have been reviewed by Steimle and Azuma,<sup>4</sup> Appelblad et al.,<sup>5</sup> and most recently by Merer.<sup>2</sup> In brief, numerous spectroscopic investigations of  $\text{CuO}$  have mapped out most of the electronic energy levels (more than 15 of them) below 25 000  $\text{cm}^{-1}$  belonging to the doublet manifold of states. Because of the restrictive  $\Delta S = 0$  selection rule and the doublet ground state ( $^2\Pi$ ) of  $\text{CuO}$ , the quartet manifold of electronic states has not generally been accessible to these investigations, with the exception of two assignments to  $^4\Sigma$  states.<sup>2</sup> The large amount of experimental data concerning this rich electronic spectrum has inspired many quantum chemical calculations of the low-lying electronic states of  $\text{CuO}$ , the most recent of which<sup>6-10</sup> correctly account for the energies of the two lowest electronic states of  $\text{CuO}$ .

The experimental and theoretical work concerning the two lowest energy electronic states ( $X^2\Pi$  and  $Y^2\Sigma^+$ ) of  $\text{CuO}$  is of particular interest to this study, since these are the states accessed in the photoelectron spectrum. The  $^2\Pi$  ground state has been well characterized by rotationally resolved spectroscopy.<sup>11</sup> Inspired by their own group's prediction of an unobserved low-lying  $^2\Sigma^+$  state,<sup>6</sup> Lefebvre et al.<sup>12</sup> searched for and observed the first excited electronic state of  $\text{CuO}$  in infrared emission ( $T_0 = 7865$  (10)  $\text{cm}^{-1}$ ). Despite the lack of rotational and vibrational resolution, the vibrational frequency of the  $Y^2\Sigma^+$  state was estimated to be 680  $\text{cm}^{-1}$  from the separation of  $\Delta\nu$  sequences. The  $Y^2\Sigma^+$  state was independently predicted by Bagus et al.<sup>7</sup> to lie at 8320  $\text{cm}^{-1}$  in a CI calculation. This calculation and others<sup>8,9</sup> indicated that the X and Y states of  $\text{CuO}$  correspond to a  $\text{Cu}^+(3d^{10})\text{O}^-(2p^5)$  ionically bound electronic configuration; the  $X^2\Pi$  state corresponds to an  $\text{O}^- 2p\sigma^2\pi^3$  ( $\pi$  hole) orbital occupancy, while the  $Y^2\Sigma^+$  possesses an  $\text{O}^- 2p\sigma^1 2p\pi^4$  ( $\sigma$  hole) configuration. However, more recent CPF (coupled pair formalism) calculations<sup>10</sup> suggest that significant configuration mixing with the  $\text{Cu}^+(3d^9 4s^1)$  occupation occurs, resulting in considerable covalent character in the bonding. These more recent calculations provided better agreement with the experimentally measured dissociation energy<sup>13</sup> and  $^2\Pi$  state

equilibrium bond length.<sup>11</sup> These calculations also yielded a much more accurate prediction of the ground-state dipole moment (4.27 D vs 7.15 D in the more ionic predictions<sup>8</sup>), subsequently measured by Steimle et al.<sup>14</sup> to be 4.45 (30) D. This experimentally measured dipole moment clearly demonstrates significant covalent contributions to the bonding in  $\text{CuO}$ .

In contrast to neutral  $\text{CuO}$ , virtually nothing is known about the  $\text{CuO}^-$  anion, with the exception of its previous mass spectrometric detection.<sup>15</sup> In this work we report the 351-nm photoelectron spectrum of  $\text{CuO}^-$ , measuring the electron detachment energy, bond length, and vibrational frequency of  $\text{CuO}^-$ . The photoelectron spectrum accesses the two lowest energy electronic states of  $\text{CuO}$ , yielding a measurement of the vibrational frequency and bond length of the  $Y^2\Sigma^+$  state.

## Experimental Section

Since the photoelectron spectroscopic technique and apparatus have been previously described in detail,<sup>16</sup> only a brief description is given here. Negative ions are produced in a copper cathode discharge source.<sup>17</sup> To produce  $\text{CuO}^-$ , a dc discharge is struck between a copper cathode at -2 to -4 kV and the chamber walls. The primary gas in the discharge is helium (0.4 Torr, flow rate = 5 SLPM) with trace amounts of argon to promote sputtering and trace oxygen to form oxides such as  $\text{CuO}^-$ . The ions formed

(1) Huber K. P.; Herzberg, G. *Molecular Spectra and Molecular Structure IV. Constants of Diatomic Molecules*; Van Nostrand Reinhold: New York, 1979.

(2) Merer, A. J. *Annu. Rev. Phys. Chem.* **1989**, *40*, 407-438.

(3) Andersen, T.; Lykke, K. R.; Neumark, D. M.; Lineberger, W. C. *J. Chem. Phys.* **1987**, *86*, 1858-1867. Engelking, P. C.; Lineberger, W. C. *J. Chem. Phys.* **1977**, *66*, 5045-5058.

(4) Steimle, T. C.; Azuma, Y. *J. Mol. Spectrosc.* **1986**, *118*, 237-247.

(5) Appelblad, O.; Lagerqvist, A.; Renhorn, I.; Field, R. W. *Phys. Scr.* **1981**, *22*, 603-608.

(6) Schamps, J.; Pinchemel, B.; Lefebvre, Y.; Raseev, G. *J. Mol. Spectrosc.* **1983**, *101*, 344-357.

(7) Bagus, P. S.; Nelin, C. J.; Bauschlicher, C. W., Jr. *J. Chem. Phys.* **1983**, *79*, 2975-2981.

(8) Igel, G.; Wedig, U.; Dolg, M.; Fuentealba, P.; Preuss, H.; Stoll, H.; Frey, R. *J. Chem. Phys.* **1984**, *81*, 2737-2740.

(9) Madhavan, P. V.; Newton, M. D. *J. Chem. Phys.* **1985**, *83*, 2337-2347.

(10) Langhoff, S. R.; Bauschlicher, C. W. *Chem. Phys. Lett.* **1986**, *124*, 241-247.

(11) Appelblad, O.; Lagerqvist, A. *Phys. Scr.* **1974**, *10*, 307-324.

(12) Lefebvre, Y.; Pinchemel, B.; Delaval, J. M.; Schamps, J. *Phys. Scr.* **1982**, *25*, 329-332.

(13) Smoes, S.; Mandy, F.; Vander Auwera-Mahieu, A.; Drowart, J. *Bull. Soc. Chim. Belg.* **1972**, *81*, 45-56.

(14) Steimle, T. C.; Nachman, D. F.; Fletcher, D. A. *J. Chem. Phys.* **1987**, *87*, 5670-5673.

(15) Leopold, D. G.; Ho, J.; Lineberger, W. C. *J. Chem. Phys.* **1987**, *86*, 1715-1726.

(16) Ervin, K. M.; Ho, J.; Lineberger, W. C. *J. Chem. Phys.* **1989**, *91*, 5974-5992.

(17) Ho, J.; Ervin, K. M.; Lineberger, W. C. *J. Chem. Phys.* **1990**, *93*, 6987-7002.

<sup>†</sup>Contribution from the Fall 1990 Experimental Physical Chemistry Laboratory Class. The following members of the class made essential contributions to the work reported here: Richard S. Blagg, John C. Brennan, David R. Carter, Clarke R. Conant, Robert D. Culp, Craig S. Dever, Garrett R. Domolky, Richard A. Heim, Margarette C. Hermann, Maxim Khaytus, Wanda S. K. Leong, Erik, T. Lloyd, Gregg H. Mac Donald, Mai H. Nguyen, Jeffrey C. Plummer, and Thomas J. Zuzelski.

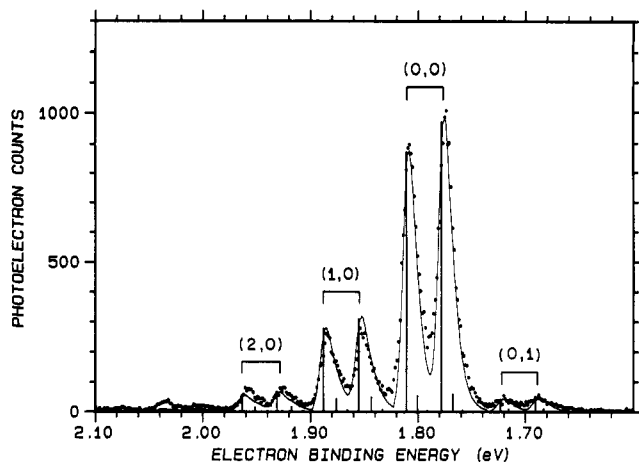


**Figure 1.** Photoelectron spectrum showing transitions from ground-state  $\text{CuO}^-$  to ground-state  $\text{CuO}(X^2\Pi)$ . Each vibrational transition is split into two components by the  $\text{CuO } ^2\Pi$  spin-orbit splitting. The experimental data are shown as points, the fit to the spectrum is shown as a solid curve, and the rotationless origins of each vibrational line are illustrated as solid vertical lines.

are allowed to equilibrate with the buffer gas in a  $1/4$ -m flow tube following the discharge. The negative ions formed in this source are extracted, focused, and accelerated to form an ion beam and are mass-selected in a Wien filter. A typical  $\text{CuO}^-$  current after mass selection was 1.5 pA. The ion beam is then decelerated into the laser interaction region, where it is crossed with a continuous laser beam ( $h\nu = 3.531$  eV) which is provided by an argon ion laser. The photodetachment signal is enhanced by enclosing the laser interaction region in a high-finesse optical cavity which provides internal powers of 30–60 W from injected laser powers of 150–200 mW.

Electrons emitted perpendicular to the crossed beams are collected in a hemispherical electron energy analyzer which has a resolution of 8–10 meV. The recorded spectrum is converted to an absolute electron kinetic energy (eKE) scale by calibration against  $\text{O}^-$ , a simultaneously produced ion of precisely known<sup>18</sup> electron affinity. A kinetic energy compression factor of approximately 0.5% is also included in the conversion of the data. This factor is an empirical correction to the relative energy scale, which was determined by measuring accurately known<sup>19</sup> Cu atomic energy level splittings in the  $\text{Cu}^-$  photoelectron spectrum. This calibration procedure enables measurement of absolute electron kinetic energies to an accuracy of  $\pm 5$  meV.

Because the electron collection angle is fixed, the angular dependence of the photodetachment cross section can be studied by rotating the laser polarization with a half-wave plate. For the spectra shown in Figure 1, the laser polarization is set at the "magic angle" such that the spectral intensities are proportional to average photodetachment cross sections. The relative peak intensities are then independent of the angular distribution, so that they can be used for a Franck-Condon analysis. The angular dependence of a photodetachment cross section is given by<sup>20</sup>

$$d\sigma/d\Omega = (\sigma_0/4\pi)[1 + (\beta/2)(3 \cos^2 \theta - 1)] \quad (1)$$

where  $\theta$  is the angle between the laser polarization vector and the direction of electron ejection and  $\beta$  is the asymmetry parameter ( $-1 \leq \beta \leq 2$ ). In order to measure  $\beta$  for each transition, the photoelectron spectrum was measured at  $\theta = 0^\circ$  and  $\theta = 90^\circ$ . To determine  $\beta$  accurately for one peak, the angular dependence of the largest peak in the spectrum was carefully measured in  $10^\circ$  intervals, and the observed intensities were least squares fit to eq 1. This accurately determined  $\beta$  could then be used to scale the  $\theta = 0^\circ$  and  $\theta = 90^\circ$  spectra with respect to one another.

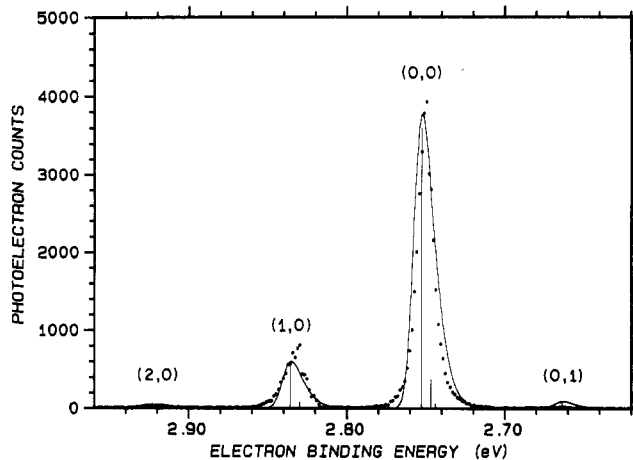


**Figure 2.** Photoelectron spectrum showing transitions from ground-state  $\text{CuO}^-$  to the first excited state of  $\text{CuO}(Y^2\Sigma^+)$ . It is illustrated in the same manner as for Figure 1.

### Results and Analysis

Figures 1 and 2 display the photoelectron spectrum of  $\text{CuO}^-$  obtained with a photon energy of 3.531 eV and plotted in terms of electron binding energy ( $h\nu - e\text{KE}$ ). The entire electron kinetic energy region of 0.10 eV up to the photon energy was searched; however, only the regions shown in Figures 1 and 2 displayed any photoelectron signal. The series of peaks in Figure 1 were assigned as vibrational transitions from the anion ground state to the  $^2\Pi$  ground state of the neutral. The  $\text{CuO}$  spin-orbit splitting and vibrational frequency evident in the photoelectron spectrum are consistent with the values measured by Appelblad et al.<sup>11</sup> for the  $^2\Pi$  state, confirming this assignment. The vibrational progression in Figure 2 was assigned as a transition from the anion ground state to the  $Y^2\Sigma^+$  state of  $\text{CuO}$  based on the origin binding energy lying  $7880 \text{ cm}^{-1}$  above the ground-state binding energy, in good agreement with previous measurements.<sup>12</sup>

Franck-Condon analyses of the vibrational progressions were employed to determine the magnitudes of the bond length changes involved in the photodetachment transitions; however, the direction of the bond length changes could not be determined from the analysis. In the analysis, the anion ground-state bond length was constrained to be smaller than that of the neutral ground state ( $^2\Pi$ ), because the larger vibrational frequency ( $739 \text{ cm}^{-1}$  vs  $640 \text{ cm}^{-1}$ ) of the anion and the experimentally determined dissociation energy (from thermochemical cycle, see below) indicate that the anion is more strongly bound than the neutral. Similarly, one expects the bond length of the neutral  $Y^2\Sigma^+$  state to fall between that of the anion and neutral ground states because of its intermediate vibrational frequency ( $680 \text{ cm}^{-1}$ ); constraining the bond length to be larger than that of the anion ground state leads to a result that is consistent with these expectations.

A Franck-Condon analysis of the vibrational progression in Figure 1 was performed as follows. The diatomic potential functions were modeled as Morse oscillators; the neutral Morse parameters are fixed along with the neutral spin-orbital splitting ( $279 \text{ cm}^{-1}$ ) at the literature values,<sup>11</sup> while the anion parameters ( $r_e, \omega_e, \omega_e x_e$ ) are allowed to vary. Franck-Condon factors are determined by numerical integration of the Laguerre wave function solutions<sup>21</sup> to the Morse potential. The rotational contours of each transition are modeled<sup>22</sup> as a convolution of the instrumental function (a Gaussian with 10 meV fwhm) with a rigid-rotor rotational spectrum at 1200 K. The unusually high rotational temperature was necessary to account for the observed line width (15 meV fwhm) and is likely due to rotational heating of the ions in the extraction process because exceptionally high extraction voltages (10–20 V) were required for this particular experiment. Because we believe the ground state of  $\text{CuO}^-$  to be  $^1\Sigma^+$  (see Discussion), the rotational spectrum was simulated as a perpen-

(18) Neumark D. M.; Lykke, K. R.; Andersen, T.; Lineberger, W. C. *Phys. Rev. A* **1985**, *32*, 1890–1892.

(19) Moore, C. E. *Atomic Energy Levels; Natl. Std. Ref. Ser., NBS 457*; US Government Printing Office: Washington, DC, 1958.

(20) Cooper, J.; Zare, R. N. *J. Chem. Phys.* **1968**, *48*, 942–943.

(21) Cashion, K. J. *Mol. Spectrosc.* **1963**, *10*, 182–231.

(22) Ervin, K. M.; Linberger, W. C. *J. Phys. Chem.* **1991**, *95*, 1167–1177.

**TABLE I: Constants for the States of CuO and CuO<sup>-</sup> Accessed in the Photoelectron Spectrum (Uncertainties Included Only for Those Constants Determined in This Work)**

constant	CuO <sup>-</sup> (X)	CuO(X <sup>2</sup> Π) <sup>a</sup>	CuO(Y <sup>2</sup> Σ <sup>+</sup> )
$T_0$ , cm <sup>-1</sup>	-14332 (48)	0	7880 (48)
$r_e$ , Å	1.670 (10) <sup>b</sup>	1.7244 <sup>c</sup>	1.704 (10) <sup>b</sup>
$\omega_e$ , cm <sup>-1</sup>	739 (25)	640.17 <sup>c</sup>	682 (25)
$\omega_e x_e$ , cm <sup>-1</sup>	$d$	4.43 <sup>c</sup>	$d$

<sup>a</sup> Spin-orbit constant fixed at ref 11 value of 279 cm<sup>-1</sup>. <sup>b</sup> Directions of bond length changes were assumed as explained in text. <sup>c</sup> Fixed at ref 11 value. <sup>d</sup> Could not be determined in fit.

dicular (Π-Σ) transition. The modeling of the rotational contour is necessary to properly account for the difference (5 meV) between the peak center and the true rotationless origin.

The following parameters were allowed to vary in a least-squares fit to the data: the anion Morse parameters, the (0,0) position and peak height, and the vibrational temperature of the negative ion. The constants determined in the fit are listed in Table I, and the resulting simulated spectrum is illustrated in Figure 1. The error bars of the parameters given are determined from examining the change in  $\chi^2$  of the fit as the parameters are fixed at different values; these error bars approximately represent a 2 $\sigma$  level of uncertainty. Because only one vibrational hot band is observed ( $T_{\text{vib}} = 500$  K), the anharmonicity of the anion could not be determined; the large error limits on the harmonic vibrational frequency in Table I partially reflect this. The adiabatic electron affinity of CuO can be determined from

$$EA(\text{CuO}) = h\nu(\text{laser}) - eKE(0,0) \quad (2)$$

to be 1.777 (6) eV.

The Franck-Condon analysis for the spectrum in Figure 2 was carried out by fixing the anion Morse parameters and vibrational temperature at the values determined in the previous fit. The constants determined in this fit for the Y<sup>2</sup>Σ<sup>+</sup> state are listed in Table I; the simulated spectrum is shown in Figure 2. It should be noted that our choice for the direction of the bond length change in this fit is based *solely* on the change in vibrational frequency. While we feel that this is the best choice given the limited information available, independent confirmation would require the observation of the Y<sup>2</sup>Σ<sup>+</sup> state with rotational resolution.

The adiabatic dissociation energy of CuO<sup>-</sup> (CuO<sup>-</sup> → Cu(2S) + O<sup>-</sup>(2P)) can be determined from

$$D_0(\text{CuO}^-) = D_0(\text{CuO}) - EA(\text{O}^-) + EA(\text{CuO}) \quad (3)$$

The dissociation energy of CuO has been determined to be 2.79 (15) eV from mass spectrometric measurements of high-temperature equilibria,<sup>13</sup> and the electron affinity of O<sup>-</sup> (1.461 122 (3) eV) has been determined from photodetachment threshold measurements.<sup>18</sup> Using the value for EA(CuO) obtained from this work, we obtain  $D_0(\text{CuO}^-) = 3.11$  (15) eV (72 (3) kcal/mol). The accuracy of this dissociation energy is clearly limited by the mass spectrometric determination of  $D_0(\text{CuO})$ . A quantity we measure very accurately is

$$D_0(\text{CuO}^-) - D_0(\text{CuO}) = 0.316$$
 (6) eV (7.29 (14) kcal/mol)

clearly demonstrating that CuO<sup>-</sup> is more strongly bound than CuO.

Finally, the polarization measurements determined  $\beta$  for each electronic state; no vibrational dependence of  $\beta$  was measurable. For detachment to the <sup>2</sup>Π ground state  $\beta$  was measured to be 0.35 (10), and for the <sup>2</sup>Σ<sup>+</sup> excited state  $\beta = 1.5$  (2).

## Discussion

In the ensuing discussion, we attempt to explain the experimentally observed bond length changes and photoelectron angular distributions in terms of simple molecular orbital concepts. It is firmly established<sup>2</sup> that the X<sup>2</sup>Π and Y<sup>2</sup>Σ<sup>+</sup> states of CuO are well described by  $\sigma^2\pi^3$  ( $\pi$  hole) and  $\sigma^1\pi^4$  ( $\sigma$  hole) configurations. Assuming a simple one-electron process for photodetachment, this would suggest a  $\sigma^2\pi^4$ (<sup>1</sup>Σ<sup>+</sup>) CuO<sup>-</sup> ground state. We find that this

configuration is the most likely ground state for CuO<sup>-</sup>.

The lowest lying dissociation asymptotes of CuO<sup>-</sup> correspond to the ground-state atoms: Cu(2S,3d<sup>10</sup>4s<sup>1</sup>) + O<sup>-</sup>(<sup>2</sup>P,2p<sup>3</sup>) and the 0.23 eV higher energy asymptote Cu<sup>-</sup>(1S,3d<sup>10</sup>4s<sup>2</sup>) + O(<sup>3</sup>P,2p<sup>4</sup>). Besides being higher in energy, the Cu<sup>-</sup> + O asymptote is not favorable for bonding, because of the closed-shell configuration of Cu<sup>-</sup>. This leaves the Cu + O<sup>-</sup> asymptote, which from can form <sup>1,3</sup>Σ<sup>+</sup> and <sup>1,3</sup>Π states.

The molecular orbital configurations of these states are described in an ab initio study by Bauschlicher and Langhoff<sup>23</sup> on the isoelectronic species ZnO, which has an isoelectronic asymptote to that of CuO<sup>-</sup>: Zn<sup>+</sup>(2S) + O<sup>-</sup>(2P). The Σ states correspond to a  $p\sigma$  hole on the oxygen, which couples to the copper 4s to yield either a singlet state with a covalent bond or a triplet state:

$$\begin{aligned} {}^1\Sigma^+ &: 3d^{10}(4s + 2p\sigma)^2 2p\pi^4 \\ {}^3\Sigma^+ &: 3d^{10} 2p\pi^4 4s^1 2p\sigma^1 \end{aligned} \quad (4)$$

Likewise, the Π states correspond to a  $p\pi$  hole on the oxygen with the configuration

$${}^{1,3}\Pi: 3d^{10} 2p\sigma^2 4s^1 2p\pi^3 \quad (5)$$

For ZnO, the bonding of these states can be described in terms of a covalent picture for the <sup>1</sup>Σ<sup>+</sup> state and in terms of an ionic picture (Zn<sup>+</sup>O<sup>-</sup>) for the other three electronic states. The ab initio calculations of ZnO predict a <sup>1</sup>Σ<sup>+</sup> ground state; however, the <sup>3</sup>Π state is of only slightly higher energy (209 cm<sup>-1</sup>). Electrostatic interactions favor the ionic <sup>3</sup>Π state, while diminished Pauli repulsion favors the more covalent <sup>1</sup>Σ<sup>+</sup> state, and these effects are of comparable magnitude. In the case of CuO<sup>-</sup>, one expects the electrostatic interaction to be greatly diminished—to first approximation the electrostatic term for the <sup>3</sup>Π state of CuO<sup>-</sup> results only from an ion-neutral interaction. Therefore, for CuO<sup>-</sup>, the <sup>1</sup>Σ<sup>+</sup> state is the most likely ground state and this state is even more heavily favored than in the case of ZnO.

Starting with the ground-state configuration of CuO<sup>-</sup>, 3d<sup>10</sup>(4s + 2pσ)<sup>2</sup>2pπ<sup>4</sup>, detachment of a  $p\pi$  electron results in a  $\sigma^2\pi^3$  <sup>2</sup>Π CuO configuration, and detachment of a  $\sigma$  electron results in a  $\sigma^1\pi^4$  <sup>2</sup>Σ<sup>+</sup> state. The experimental results show that both orbitals are slightly bonding; detachment of the  $\pi$  electron results in a 0.05-Å increase in bond length, while detachment of the  $\sigma$  electron yields a 0.03-Å increase. The simple single-configuration picture we are using would indicate that the  $\pi$  orbital is nonbonding and the  $\sigma$  orbital is bonding; however, ab initio calculations on isoelectronic ZnO<sup>23</sup> indicate that O<sup>-</sup> 2pπ donation to the metal-centered 4pπ orbitals plays a significant role (4pπ occupancy as high as 0.54) in the bonding of the <sup>1</sup>Σ<sup>+</sup> state, suggesting the same could be true for CuO<sup>-</sup>. Furthermore, the large spin-orbit constant measured for the X<sup>2</sup>Π state of CuO (279 cm<sup>-1</sup>) indicates that the  $\pi$  electron cannot be completely localized on the oxygen.<sup>2</sup>

The observed photoelectron angular distributions are consistent with this picture. For photodetachment near threshold (eKE < 2–4 V), detachment from an s-like orbital causes electron ejection parallel to the laser polarization to be favored ( $\beta$  positive), while detachment from higher angular momentum orbitals results in more isotropic or perpendicular ejection ( $\beta$  close to 0 or negative).<sup>20</sup> The observed  $\beta$  of 1.5 (parallel ejection is favored 10-fold over perpendicular) for detachment to the Y<sup>2</sup>Σ<sup>+</sup> state is consistent with detachment from the (4s + 2p)σ orbital, because of the large  $\sigma$  contribution to the orbital. The relatively isotropic distribution ( $\beta = 0.35$ ) observed for detachment to the X<sup>2</sup>Π state is not consistent with detachment from a completely oxygen-centered nonbonding O<sup>-</sup> orbital, since photodetachment studies<sup>24</sup> of O<sup>-</sup> have shown that detachment of an O<sup>-</sup> 2p electron with 1.7 eV energy should yield  $\beta = -0.8$ . This is in good agreement with the observed geometry change (+0.054 Å) and dissociation energy change (-0.36 eV) which both show that the detachment orbital cannot

(23) Bauschlicher, C. W., Jr.; Langhoff, S. R. *Chem. Phys. Lett.* **1986**, *126*, 163–168.

(24) Hanstorp, D.; Bengtsson, C.; Larson, D. J. *Phys. Rev. A* **1989**, *40*, 670–675.

be entirely nonbonding; in fact, the experimentally measured geometry changes would indicate that it is at least as bonding as the  $\sigma$  orbital.

Finally, it must be noted that the preceding description is likely an oversimplification. Because of a closed-d-shell ( $3d^{10}$ ) configuration, CuO and  $\text{CuO}^-$  are more simply described than most transition-metal oxides; nevertheless, the details of the bonding in CuO have been the subject of some controversy. Our simplified picture is, however, sufficient to account for the essential features of the information available in the photoelectron spectrum, suggesting that it is a satisfactory first-order description.

### Conclusion

Photoelectron spectroscopy has been used to measure transitions from the  $\text{CuO}^-$  ground state to the two lowest lying electronic

states of neutral CuO, the  $X^2\Pi$  and  $Y^2\Sigma^+$  states. The electron affinity of ground-state CuO was determined to be 1.777 (6) eV. Franck-Condon analyses of the vibrational progressions in both electronic transitions were used in conjunction with previously determined<sup>11</sup> spectroscopic parameters for the CuO ground state, to determine previously unknown vibrational frequencies and bond lengths for the  $\text{CuO}^-$  ground state and the first excited state of  $\text{CuO}(Y^2\Sigma^+)$ . Our results can be explained in terms of detachment from a  $^1\Sigma^+ \text{CuO}^-(\sigma^2\pi^4)$  ground state to the  $\text{CuO } X^2\Pi$  ( $\pi$  hole) and  $Y^2\Sigma^+$  ( $\sigma$  hole) states.

*Acknowledgment.* This work was carried out as a class project in the Fall 1990 Experimental Physical Laboratory course. The work was supported by National Science Foundation Grants PHY90-12244 and CHE88-19444.

## <sup>1</sup>H NMR Procedure To Estimate the Extent of Metal Surface Covered by $\text{TiO}_x$ Overlayers in Reduced Rh/ $\text{TiO}_2$ Catalysts

J. P. Belzunegui, J. M. Rojo,\* and J. Sanz

*Instituto Ciencia de Materiales, CSIC, C/Serrano 115 dpdo, 28006-Madrid, Spain  
(Received: February 21, 1991)*

Oxidation at different temperatures of an Rh/ $\text{TiO}_2$  sample in the SMSI state has been studied by <sup>1</sup>H NMR spectroscopy. In the range 273–473 K electronic perturbation of the metal is progressively eliminated. However, removing of  $\text{TiO}_x$  species, which block physically the metal adsorption sites, requires oxidation at 673 K. At this temperature metal particles recover their maximum hydrogen adsorption capacity. From the difference between adsorbed hydrogen in the sample oxidized at 473 and 673 K, a measurement of the metal surface covered by  $\text{TiO}_x$  species has been obtained. The influence of reduction pretreatments (temperature and time) on the degree of  $\text{TiO}_x$  coverage has been also analyzed.

Reduction under flowing  $\text{H}_2$  at 773 K of catalysts formed by group VIII noble metal supported on  $\text{TiO}_2$  inhibits  $\text{H}_2$  and CO adsorption on the metal. This phenomenon was first ascribed to a strong metal-support interaction (SMSI).<sup>1,2</sup> The two most accepted causes for the SMSI state are (i) coverage by titanium suboxide ( $\text{TiO}_x$ ,  $1 < x < 2$ ) species of metal particles and (ii) formation of bondings between titanium cations and metal atoms.<sup>1-15</sup> Recently, it has been shown<sup>16</sup> in Rh/ $\text{TiO}_2$  catalysts that

the SMSI state is established in two consecutive stages: one when the catalyst is reduced in the range 373–673 K and the other for reduction temperatures above 673 K. In the first stage, the metal adsorption loss was related to incorporation of hydride-like species into the metal-support interface while, in the second one, formation of rhodium-titanium bondings and coverage by  $\text{TiO}_x$  species of metal particles have been proposed to explain experimental data. A  $\text{TiO}_x$  overlayer on metal particles has been observed<sup>7</sup> by HRTEM in Rh/ $\text{TiO}_2$  catalysts reduced in  $\text{H}_2$  at 773 K. However, information concerning hydrogen adsorption suppression due to physical blocking of metal adsorption sites by that overlayer in real catalysts is still limited. In this work, we have investigated by <sup>1</sup>H NMR spectroscopy elimination of SMSI state by oxidation of an Rh/ $\text{TiO}_2$  sample at increasing temperatures. From analysis of NMR spectra corresponding to the sample oxidized at 473 K after different reduction treatments, a measurement of the metal surface covered by  $\text{TiO}_x$  species has been obtained.

The catalyst Rh(2.5 wt %)/ $\text{TiO}_2$  was prepared by the incipient wetness method described elsewhere.<sup>17</sup> Metal particle sizes are in the range 2–10 nm. Thermal treatments of the sample up to 773 K were performed in Pyrex tubular cells with high-vacuum stopcocks. The catalyst reduced in flowing  $\text{H}_2$  at 773 K for 1 h is called hereafter H. Two types of experiments were done: (i)

(1) Tauster, S. J.; Fung, S. C.; Garten, L. R. *J. Am. Chem. Soc.* **1978**, *100*, 170.

(2) Tauster, S. J.; Fung, S. C.; Baker, R. T. K.; Horsley, J. A. *Science* **1981**, *211*, 1121.

(3) Belton, D. N.; Sun, Y.-M.; White, J. M. *J. Am. Chem. Soc.* **1984**, *106*, 3059.

(4) Sun, Y.-M.; Belton, D. N.; White, J. M. *J. Phys. Chem.* **1986**, *90*, 5178.

(5) Sadeghi, H. R.; Henrich, V. E. *J. Catal.* **1984**, *87*, 279.

(6) Sanchez, M. G.; Gazquez, J. L. *J. Catal.* **1987**, *104*, 120.

(7) Logan, A. D.; Braunschweig, E. J.; Dartye, A. K.; Smith, D. J. *Langmuir* **1988**, *4*, 827.

(8) Munuera, G.; González-Elipe, A. R.; Espinós, J. P.; Conesa, J. C.; Soria, J.; Sanz, J. *J. Phys. Chem.* **1987**, *91*, 6625.

(9) Levin, M.; Salmeron, M.; Bell, A. T.; Somorjai, G. A. *Surf. Sci.* **1986**, *169*, 123.

(10) Ko, C. S.; Gorte, R. J. *Surf. Sci.* **1985**, *161*, 597.

(11) Koningsberger, D. C.; Martens, J. H. A.; Prins, R.; Short, D. R.; Sayers, D. E. *J. Phys. Chem.* **1986**, *90*, 3047.

(12) Martens, J. H. A.; Prins, R.; Zandbergen, H.; Koningsberger, D. C. *J. Phys. Chem.* **1988**, *92*, 1903.

(13) Sakellson, S.; McMillan, M.; Haller, G. L. *J. Phys. Chem.* **1986**, *90*, 1733.

(14) Resasco, D. E.; Weber, R. S.; Sakellson, S.; McMillan, M.; Haller, G. L. *J. Phys. Chem.* **1988**, *92*, 189.

(15) Yokoyama, T.; Asakura, K.; Iwasawa, Y.; Kuroda, H. *J. Phys. Chem.* **1989**, *93*, 8323.

(16) Belzunegui, J. P.; Sanz, J.; Rojo, J. M. *J. Am. Chem. Soc.* **1990**, *112*, 4066.

(17) Conesa, J. C.; Malet, P.; Munuera, G.; Sanz, J.; Soria, J. *J. Phys. Chem.* **1984**, *88*, 2986.